FULL TITLE
ASP Conference Series, Vol. **VOLUME**, **YEAR OF PUBLICATION**
NAMES OF EDITORS

Probing the Compact Jets of Blazars with Light Curves, Images, and Polarization

Alan P. Marscher

Institute for Astrophysical Research, Boston University, 725 Commonwealth Ave., Boston, MA 02215

Abstract. I review the outstanding questions regarding the nature of relativistic jets as well as the tools available for exploring the rich phenomena observed in blazars. Each technique provides important information, but it is only by combining the methods that we can hope to obtain a complete description of blazar jets. I advocate monitoring a number of blazars comprehensively to obtain detailed multiwaveband light curves to sample changes in the spectral energy distribution, sequences of mm-wave images with resolution $\sim$ 0.1 milliarcseconds, and polarization at as many frequencies as possible, including those at which imaging is available. Such a program has the potential of allowing us to synthesize multiwaveband emission maps from radio frequencies to γ-ray energies.

1. Introduction: Questions about Blazar Jets and Methods for Answering Them

There are few phenomena in astrophysics as exciting as relativistic jets. They emit radiation across the electromagnetic spectrum through exotic processes involving ultra-high-energy electrons embedded in magnetic fields. Their nearly luminal flow speeds create illusions of superluminal motion, radiation enhanced by Doppler beaming, and variations in brightness and polarization over times shorter than the light-crossing time of the emitting plasma.

If we wish to study relativistic jets, blazars are the handiest objects to observe. Their jets are highly relativistic and pointing nearly at us, which causes their emission to dominate over that of the less exciting, unbeamed radiation that can be found in any of the more mundane active galaxies (see Fig. 1). Of course, much can be learned by studying jets viewed side-on and especially those found in X-ray binaries, but only blazars allow us to taste the flavors of the full menu offered by highly relativistic jets.

Of course, one cannot get telescope time to observe blazars simply by pointing out that they are exciting objects. We should expect that the data we propose to collect will answer some fundamental questions that puzzle us about the nature of jets. Among these questions are:

1. How are jets made by accreting black holes?
2. How and where are jets accelerated such that they flow with high Lorentz factors?
3. How and where are the jets focused to opening angles less than a few degrees?
4. Where and how are the relativistic electrons accelerated?
5. What physical conditions exist and how do they arise? These can include

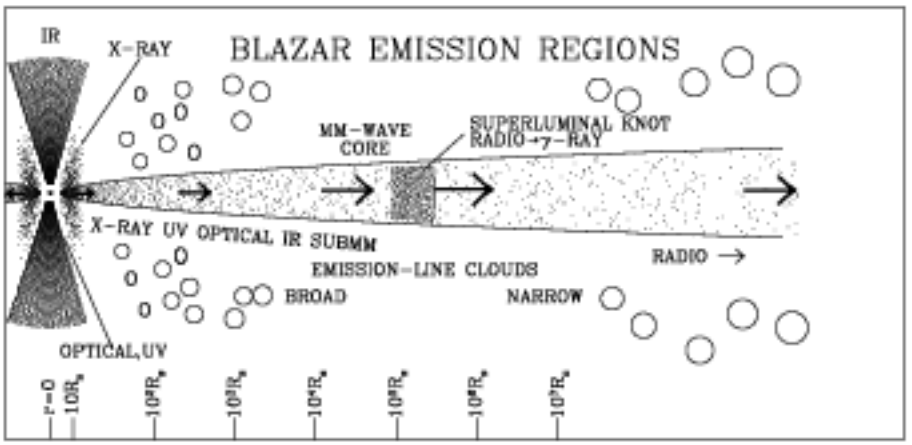

Figure 1. Rough sketch of the emission regions of a radio-loud active galaxy. Note the logarithmic scale on the bottom for the distance down the jet. The likely waveband of photons that can be emitted at each site is indicated. It remains to be determined whether there is substantial emission between the base of the jet and the mm-wave core. (Adapted from Marscher 2005.)

shocks, turbulence, instabilities, bending, precession or less regular shifts in direction, matter content (electron-proton vs. pair plasmas), magnetic field patterns, large-scale electrical currents, and interaction with the external medium. Figure 2 illustrates how a few of these physical processes may manifest themselves in blazar jets.

The techniques that are available for probing the inner workings of blazar jets are limited, mainly because the angular size scales are extremely small close to the central engine. Very long baseline interferometry (VLBI) samples scales ~ 0.1 milliarcseconds (mas) routinely at 7 mm (43 GHz) and even smaller scales at shorter millimeter wavelengths, although at the expense of dynamic range and perhaps even image fidelity. This corresponds to $\sim 10^4$ gravitational radii at the distance of 3C 273. Variability can potentially probe scales as small as the timescale of significant changes (transformed to the rest frame after correcting for redshift and Doppler boosting) multiplied by the speed of light. Light curves, however, are difficult to interpret since the timescales are related to sizes and not necessarily to distance from the central engine, plus the reason for variability is often unclear. Multiwaveband light curves improve the situation since they provide both the evolution of the spectral energy distribution (SED) and, via time lags, valuable information on the processes of energy gains and losses. Finally, polarization is an excellent probe of the degree of ordering of the magnetic field and the mean direction of the field (once the effects of aberration and Faraday rotation are removed). But the presence of different magnetic field configurations in separate emission regions often confuses rather than enlightens us.

Fortunately, it is now possible to combine these techniques, although to do so requires a lot of effort, a legion of collaborators, and a multitude of observing proposals. The Very Long Baseline Array (VLBA) produces images at 7 mm

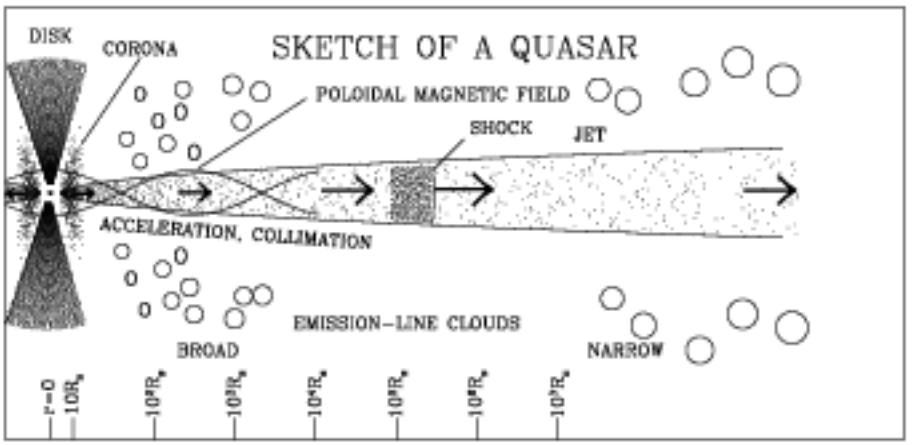

Figure 2. Sketch similar to Figure 1 but with some of the physical processes that are thought to occur inside jets. (Adapted from Marscher 2005.)

in total intensity at dynamic ranges up to $\sim$ 1000:1 and in polarized intensity with sensitivity sufficient to measure the polarization of all major emission features. One can—if the referees and scheduling committee are willing—observe as frequently as once per 1-2 months, in which case very few, if any, of the main events are missed in the sequences of images. We argue below that such monitoring of the polarization and structure can be combined with total-source polarization monitoring at shorter wavelengths to relate the emission at short millimeter, submillimeter, IR, and optical bands to events or long-lived features in the VLBA images. Adding total flux light curves at a variety of wavebands might then allow us to map the emission across the entire electromagnetic spectrum with the VLBA images providing the reference locations and motions.

Before undertaking such an ambitious program, we need to convince ourselves that the emission at different wavebands is indeed intimately related. I hope that the next section convinces the reader that this is the case.

2. Connections between Low and High Frequency Emission

2.1. Images

As is well known, sequences of milliarcsecond-scale VLBI images reveal knots of emission moving away from a "core" at superluminal apparent speeds in most blazars (e.g., Jorstad et al. 2001; Kellermann et al. 2004). Recent studies at the relatively high frequency of 43 GHz reveals considerably higher apparent speeds in many blazars than had been observed previously (Jorstad et al. 2001, 2005; Jorstad & Marscher 2005). This is due in part to the presence of stationary features that, when blended with moving knots at the coarser resolution of lower frequencies, causes confusion leading to lower derived apparent velocities than is actually the case. Of course, the same problem can afflict the 43 GHz analysis, so relying on model fitting to define positions of components that are not well

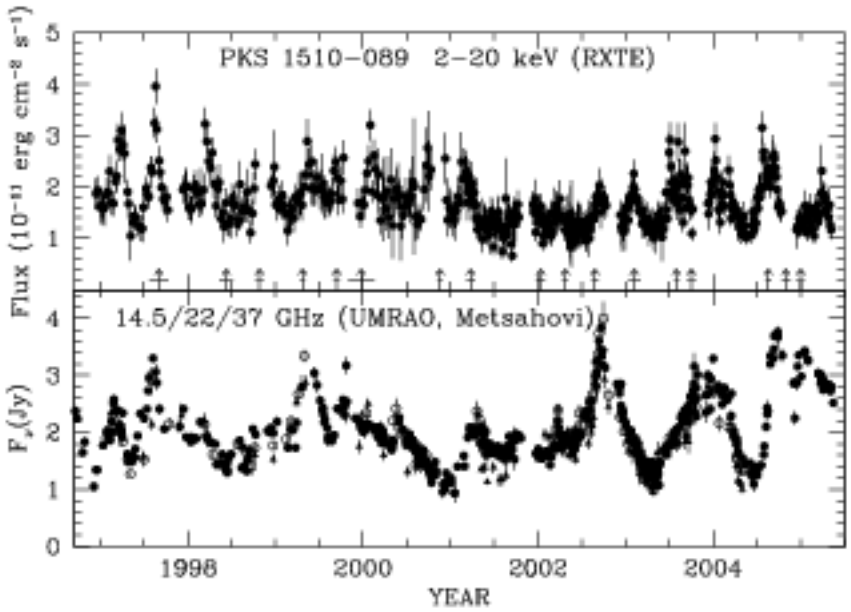

Figure 3. X-ray and radio light curves of the quasar PKS 1510−089. Arrows give times of known ejections of superluminal radio knots up to 2005.0. Data are from Marscher et al. (2004) and Marscher et al. (2006).

resolved from each other adds an extra level of uncertainty to the proper motions obtained.

At 43 GHz we often see significant changes in both structure and polarization on timescales of weeks. A monitoring frequency less than once per month can miss some of these variations and even cause one to mis-identify knots across epochs of observation. Polarization can help, but in some cases changes in the degree and direction can be quite sudden, so there is no reliable substitute for good time sampling.

2.2. Multiwaveband Light Curves

Figures 3 and 4 display multiwaveband light curves of two highly variable quasars that my collaborators and I have been monitoring, PKS 1510−089 ($z = 0.361$) and 3C 279 ($z = 0.538$). As can be seen in the figures, most X-ray flares in both sources can be associated with ejections of superluminal radio knots (see Figs. 3 and 4). The apparent speeds are extremely high: 28-46c in PKS 1510−089 (Jorstad et al. 2005) and up to 21c in 3C 279 (Jorstad & Marscher 2005). The first of these papers determines the Doppler factor by comparing the timescale of variability of knots with their sizes. This allows derivation of the Lorentz factor and angle to the line of sight (see the paper by Jorstad et al. in these proceedings). A detailed kinematic model of the changing apparent speed and direction of motion allows the same in 3C 279. Jorstad et al. (2005) conclude that the jet in PKS 1510−089 has a variable Lorentz factor that reaches 48 with a Doppler factor up to 44, while the Lorentz factor in 3C 279 is as high as 24

and the Doppler factor has a value up to 40. The very high Doppler factors explain why these are such extreme blazars.

Both inspection by eye of Figures 3 and 4 and formal analysis (Marscher et al. 2004) indicate that there is a strong correlation between the radio and X-ray variations in PKS 1510−089 and between the optical and X-ray light curves in 3C 279 (Marscher et al. 2004). In each case, the X-rays usually lag the lower-frequency emission. The cross-correlation of the entire light curves gives a radio/X-ray lag of 6 ± 6 days in PKS 1510−089 and an optical/X-ray lag of 15 ± 15 days in 3C 279, where the standard deviation cited corresponds to the FWHM of the peak in the discrete cross-correlation function (Marscher et al. 2004). The "reverse" time delays can be understood if the X-rays are from synchrotron self-Compton emission, in which case there is a light-travel delay. This occurs because the synchrotron seed photons need to move across part of the source before they are scattered, whereas the synchrotron photons propagate promptly toward the observer as the flare develops (Sokolov, Marscher, & McHardy 2004). This cannot work for shocks oriented transversely to the jet axis unless the relevant portion of the jet makes an angle $< \Gamma$ to the line of sight, which is consistent with the results of intensive VLBA monitoring of 3C 279 (Jorstad & Marscher 2005). On the other hand, in this quasar frequency stratification can also delay the peaks of X-ray flares relative to those in the optical. In the case of PKS 1510−089, Jorstad et al. (2005) find that the viewing angle $\sim \Gamma$ in 1998-99. During this period, however, the radio/X-ray correlation deviated from the radio-leads norm (see Fig. 3 and Marscher et al. 2004), so the theoretical requirement is not relevant. We are still analyzing the later VLBA data, which should allow us to determine whether times when the radio variations lead indeed correspond to smaller viewing angles.

The superluminal ejections usually correspond to radio flares in the quasar PKS 1510−089, although sometimes the rising flux of the new knot is canceled out in the light curve by the decay of the previous event. The X-ray lag (average of 6 days) implies that in this quasar the X-rays come from the radio-emitting portion of the jet. Jorstad et al. (2001) have drawn a similar conclusion regarding the γ-ray emission of blazars, based on a statistical association of superluminal ejections with high γ-ray flux states that lag behind the epoch when the radio knot coincided with the core.

In 3C 279 the X-rays lag the optical by 15 ± 15 days, so the X-rays come from near or downstream of the optically emitting region. The radio variations at 37 GHz are delayed by 140 ± 40 days relative to the X-ray light curve. Very little of this is due to opacity at 37 GHz, since there is little time delay between the 37 GHz and 90 GHz light curves. Nor is it caused completely by the flux of radio knots peaking several months after they leave the core region, since the knots that accompanied the largest outburst, in 2001, became weak by the time they were more than 0.1 mas from the core. From the parameters of knot $C19$ of Jorstad & Marscher (2005) and the time delay of 140 days we can conclude that the mm-wave core is quite far from the optical/X-ray emitting region—a deprojected distance of ~ 100 pc.

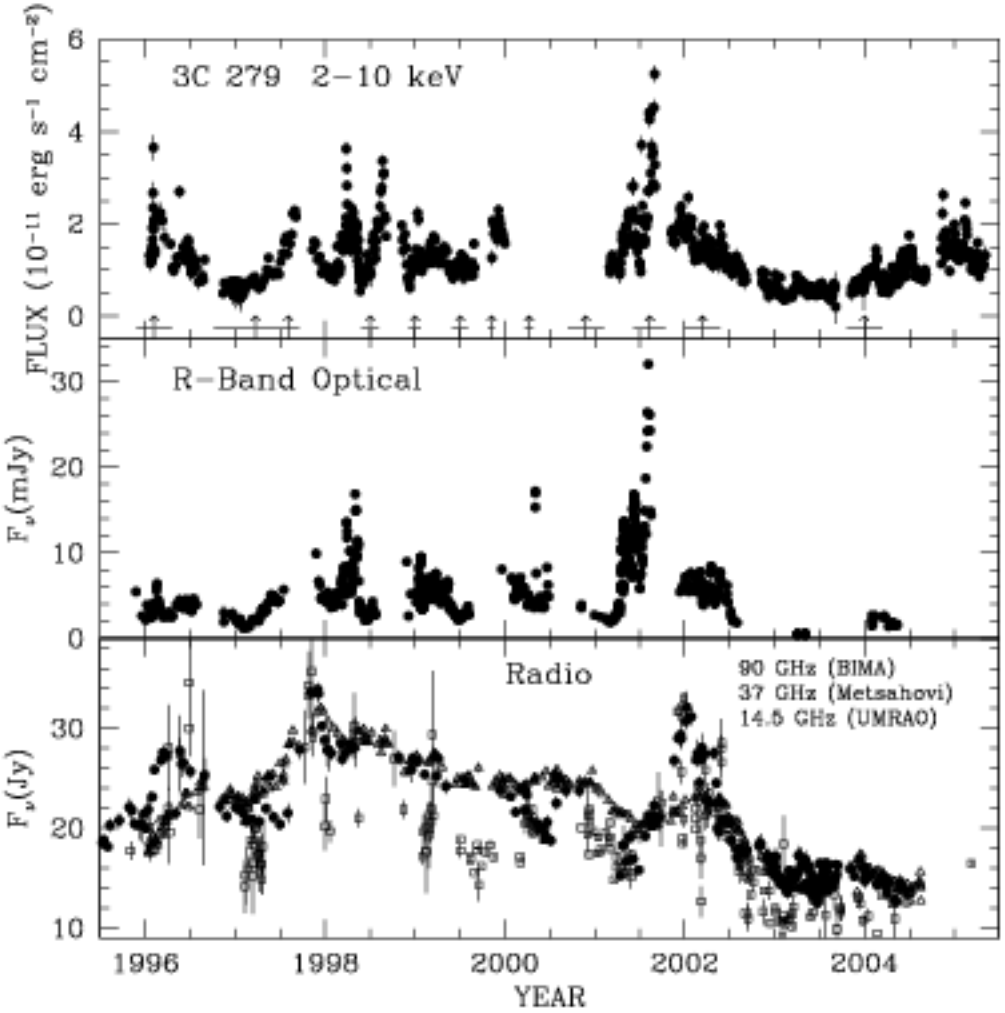

Figure 4. X-ray, optical, and radio/mm-wave light curves of 3C 279. Arrows give times of known ejections of superluminal radio knots up to 2004.3. Ejections in mid-1996 may have been missed because of gaps in the time coverage of VLBA observations. Data are from Marscher et al. (2004) and Marscher et al. (2006).

2.3. Millimeter-wave and Optical Polarization

Marscher & Jorstad (2005) show an example of similarities in the polarization electric-vector position angles (EVPAs) of some blazars at 7 mm, 1.3/0.85 mm, and optical wavelengths. The ~ 1 mm and optical EVPAs often line up with those of features seen in the VLBA images. In a number of cases we see changes in the high-frequency EVPA such that it lines up with an emerging superluminal knot seen at 7 mm. In addition, Gabuzda & Sitko (1994) and Gabuzda, Sitko, & Smith (1994) have previously reported observed relations between longer wavelength VLBI and optical polarization.

We can interpret these cross-frequency polarization similarities in a few different ways. The simplest is that the synchrotron emission from mm-wave to optical is at least partially co-spatial. This is expected, for example, in the shock-in jet models (e.g., Marscher & Gear 1985). The tendency of higher degrees of polarization to be measured at higher frequencies is then the result of the smaller volumes that contain the highest energy electrons: ordered magnetic fields can occur in small cells even if the global field is fairly chaotic. Alternatively, the same structure in the jet might be responsible for the emission at all frequencies, but at different times because the dominant frequency of emission changes as the feature propagates down the jet. This could well be the case in 3C 279 where we find optical/X-ray to mm-wave time lags of more than 100 days (see above). Another possibility is that there is a systematic ordered component to the magnetic field, for example a helical field (e.g., Lyutikov et al. 2005), in the jet that modulates the polarization of all emission regions within an extended section of the jet. In fact, this is required by models in which the jet is accelerated magnetohydrodynamically (Meier, Koide, & Uchida 2000; Vlahakis & Königl 2004). Yet another explanation is that the magnetic field geometry is arranged in a similar manner in different emission components. For example, polarization parallel to the jet occurs when a disordered field is compressed by a shock front oriented transverse to the jet axis (Laing 1980), while perpendicular polarization could correspond to shearing at a boundary layer. However, it is difficult to imagine how this idea could apply to the case of moving knots with polarization oriented obiquely to the jet direction, as is often seen.

3. Suggested Program Combining Light Curves, Images, and Polarization

One of the great problems in interpreting multiwaveband light curves is difficulty in associating high and low flux states at one frequency with those at another. Correlation analysis can do this statistically, but in order to derive physical parameters we need to know, for example, which specific flare at optical wavelengths corresponds to one seen in the radio light curves. Of course, maximizing the time coverage helps, but a one-to-one correspondence between light curves at different wavebands is rarely observed and not even expected theoretically when there is frequency stratification owing to energy losses (Sokolov, Marscher, & McHardy 2004).

I think that polarization is the key, since it can be measured alongside the light curves at optical and longer wavelengths, and can be imaged along with the total intensity by VLBI observations. The general procedure is as follows:

1. Monitor the object as frequently and at as many wavelengths as you can in total flux and, at wavebands for which it is possible, in polarization.
2. Image at one or more mm wavelengths with VLBI as often as the scheduling committee will allow. (Once per month is usually adequate, once per two months is marginal.)
3. Identify features in both the polarization light curves and the images that have identical (to within the uncertainties) electric vector position angles (EVPAs).

From the time delays between when the polarization signatures appear in the light curves and on the sequence of VLBA images, it should be possible to determine which features in the images correspond to events in the light curves. One can then construct a crude emission map of the sites of emission at different times. Even at wavebands, such as X-ray and γ-ray, where polarization observations are not currently possible, strong correlations of light curves can be used to estimate the locations of the emission regions relative to those for which polarization provides more precise information.

My collaborators and I are carrying out such a program with the VLBA (at 43 GHz), Lowell Observatory's 1.8 m Perkins Telescope (optical and IR polarization), the Crimean Astrophysical Observatory and Steward Observatory (optical polarization), the JCMT (polarization at $\lambda \sim 1$ mm), RXTE (X-ray, no polarization), and various optical telescopes without polarization capabilities. If successful, we plan to continue by adding γ-ray total-flux light curves supplied by *GLAST* after its launch, currently scheduled for 2007.

Acknowledgments. This research was funded in part by US National Science Foundation grant AST-0406865 and NASA grant NNG 04GO85G. The VLBA is an instrument of the National Radio Astronomy Observatory, a facility of the National Science Foundation operated under cooperative agreement by Associated Universities, Inc.

References

Gabuzda, D. C., & Sitko, M. L. 1994, AJ, 107, 884
Gabuzda, D. C., Sitko, M. L., & Smith, P. S. 1996, AJ, 112, 1877
Jorstad, S. G., et al. 2001, ApJS, 134, 181
Jorstad, S. G., et al. 2001, ApJ, 556, 738
Jorstad, S. G. 2005, AJ, in press
Jorstad, S. G., & Marscher, A. P. 2005, Mem. S.A.It., 76, 106
Kellermann, K. I., et al. 2004, ApJ, 609, 539
Laing, R. A. 1980, MNRAS, 193, 439
Lyutikov, M., Pariev, V. I., & Gabuzda, D. C. 2005, MNRAS, 360, 869
Marscher, A. P. 2005, Mem. S.A.It., 76, 13
Marscher, A. P. et al. 2004, in X-Ray Timing 2003: Rossi and Beyond, ed. P. Kaaret, F. K. Lamb, & J. H. Swank (Melville, NY: AIP), 167
Marscher, A. P., et al. 2006, in preparation
Marscher, A. P., & Gear, W. K. 1985, ApJ, 298, 114
Marscher, A.P., & Jorstad, S. G. 2005, in Astronomical Polarimetry: Current Status and Future Directions, ed. A. Adamson et al., ASP Conf. Ser., in press
Meier, D. L., Koide, S., & Uchida, Y. 2000, Sci, 291, 84
Sokolov, A., Marscher, A. P., & McHardy, I. M. 2004, ApJ, 613, 725
Vlahakis, N., & Königl, A. 2004, ApJ, 605, 656